Materials Science-Poland, 32(4), 2014, pp. 652-660
http://www.materialsscience.pwr.wroc.pl/
DOI: 10.2478/s13536-014-0244-7

VERSITA

Investigations on the structural, morphological, optical and electrical properties of undoped and nanosized Zn-doped CdS thin films prepared by a simplified spray technique

M. ANBARASI, V.S. NAGARETHINAM, A.R. BALU*

PG and Research Department of Physics, AVVM Sri Pushpam College, Poondi – 613 503, Tamilnadu, India

CdS and Zn-doped CdS (CdS:Zn) thin films have been deposited on glass substrates by spray pyrolysis technique using a perfume atomizer. The influence of Zn incorporation on the structural, morphological, optical and electrical properties of the films has been studied. All the films exhibit hexagonal phase with (0 0 2) as preferential orientation. A shift of the (0 0 2) diffraction peak towards higher diffraction angle is observed with increased Zn doping. The optical studies confirmed that the transparency increases as Zn doping level increases and the film coated with 2 at.% Zn doping has the maximum transmittance of about 90 %. The sheet resistance (R_{sh}) decreases as the Zn-doping level increases and a minimum value of 1.113×10^3 Ω/sq is obtained for the film coated with 8 at.% Zn dopant. The CdS film coated with 8 at.% Zn dopant has the best structural, morphological and electrical properties.

Keywords: *X-ray diffraction; crystal structure; preferential orientation; thin films; optical properties; electrical studies*

1. Introduction

CdS is a technologically important II – VI compound semiconductor with a direct optical band gap of ∼2.42 eV at room temperature. Because of its wide band gap, CdS is used as a window material for heterojunction solar cells. It also finds application in light-emitting diodes (LED) [1], gas detectors [2], photo-voltaic cells [3], nonlinear optics [4], and thin film transistors [5]. CdS shows n-type conductivity owing to its native defects or sulfur vacancies and cadmium interstitials. Therefore, it is possible to control the conductivity of CdS by controlling those native defects or alternatively by doping of CdS with some metallic ions of group III, such as indium (In^{3+}) [6], aluminium (Al^{3+}) [7], gallium (Ga^{3+}) [8] and boron (B^{3+}) [9] or with metallic ions of group II, such as cobalt (Co^{2+}) [10] and nickel (Ni^{2+}) [11]. The properties (electrical, optical and magnetic) of CdS are strongly modified by the doping of Co^{2+} and Ni^{2+} because of the sp-d exchange interaction between the localized d-electrons of the transition metal magnetic ions and the mobile carriers in the conduction or valence band [10, 11]. In general, it was observed that when the dopant ions have a radius slightly smaller than that of Cd^{2+}, the conductivity increases and the lattice unit cell compresses. Zn is an important transition metal element having an ionic radius of 0.074 nm, which is smaller than that of Cd^{2+} (0.097 nm), hence, Zn^{2+} can easily penetrate into CdS crystal lattice or substitute Cd^{2+} position in the crystal [12]. Accommodation of a wide range of Zn into the lattice of CdS can tune its energy gap and lattice parameters, which make it useful in solar cells, diodes, sensors and microelectronics applications. Considering the advantages laid down by Zn-doping of CdS thin films, we focus our work on investigation of physical properties of Zn doped CdS films in order to improve the performance of optoelectronic devices and find their new applications. High quality undoped and doped CdS semiconductor thin films have been prepared by a wide range of methods, such as thermal evaporation [13], spray pyrolysis [14], sputtering [15], pulsed laser deposition (PLD) [16], molecular beam epitaxy (MBE) [17], chemical bath deposition (CBD) [18] and electro

*E-mail: arbalu757@gmail.com

deposition (ED) [19]. Among these methods, spray pyrolysis technique is one of the most commonly used methods for preparation of high quality polycrystalline CdS films owing to its simplicity, safety, non-vacuum system of deposition, hence, inexpensive method for large area coatings [20]. In the present work, a simplified spray pyrolysis technique using a perfume atomizer [21] is employed to deposit Zn-doped CdS (CdS:Zn) thin films with different Zn doping concentrations.

2. Experimental details

2.1. Preparation of CdS:Zn films

CdS thin films were prepared from anhydrous cadmium chloride ($CdCl_2 \cdot H_2O$) and thiourea ($CS(NH_2)_2$) dissolved in 50 ml of deionized water. Zinc chloride, $ZnCl_2$ was added to the starting solution for zinc doping in a concentration of 0, 2, 4, 6 and 8 at.% Zn. The solution was stirred thoroughly using a magnetic stirrer for 30 min and then sprayed manually using a perfume atomizer on preheated glass substrates kept at 400 °C. Before the deposition process, the glass substrates were degreased with organic solvent, rinsed with deionized water and dried in air.

2.2. Characterization

The as deposited films were yellow, uniform, pinhole free and strongly adherent to the glass substrates. The layer thickness was measured by gravimetric weight difference method using a sensitive microbalance. The thickness of CdS:Zn films was found to vary from 510 nm to 680 nm with an accuracy of 5 %. The structure, crystallinity and phase of CdS and Zn-doped CdS thin films were determined with a X-ray diffractometer (XPERT-PRO model), using CuKα radiation ($\lambda = 1.5406$ Å) with 2θ ranging from 20° to 80°. The surface morphology and composition of the films were characterized by scanning electron microscopy (SEM) and energy dispersive X-ray analysis (EDAX) with the help of JEOL-JSM Japan. UV-Vis-NIR spectrophotometer (SHIMADZU UV-1700) was used to record the optical absorption spectra of the samples in the wavelength range of 300 to 1100 nm. Electrical resistivity measurement was done using DC two point probe method in the 303 to 403 K temperature range in steps of 5 K.

3. Results and discussion

3.1. Structural analysis

X-ray diffraction (XRD) patterns of the undoped and Zn-doped spray deposited CdS films are shown in Fig. 1.

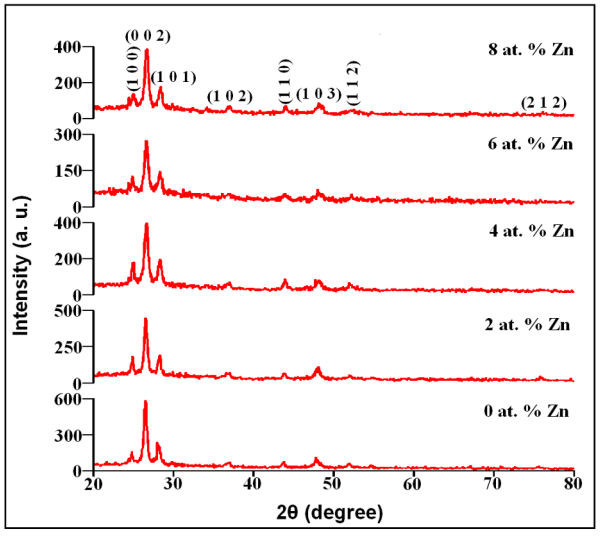

Fig. 1. XRD patterns of undoped and Zn-doped CdS thin films.

The diffraction peaks show that the films have polycrystalline nature of hexagonal phase, with (0 0 2) preferred orientation, irrespective of the Zn doping level, which indicates that the incorporation of Zn into the Cd sites has not altered the preferential growth. The other peaks observed at $2\theta =$ 24.7°, 28.15°, 36.7°, 43.7°, 47.8° and 51.9° can be indexed to (1 0 0), (1 0 1), 1 0 2), (1 1 0), (1 0 3) and (1 1 2) planes of pure CdS (JCPDS Card No. 06-0314). No peaks related to ZnS are observed in the patterns, indicating the purity of the films. The predominance of the (0 0 2) plane in all the films clearly shows that the growth of the crystal was such that the c-axis was perpendicular to the surface of the substrate. Our previous work on CdS thin films fabricated at different substrate temperatures showed a similar preferential orientation [22].

Hexagonal CdS thin films with preferential orientation along the (0 0 2) plane was also reported by Wilson et al. [23].

Crystallites in a polycrystalline material normally have a crystallographic orientation different from that of their neighbours. This orientation of the crystallites called the preferential orientation may be randomly distributed with respect to some selected frame of reference. The preferential orientation factor f(h k l) for the (0 0 2) plane is calculated relative to the other observed peaks by evaluating the fraction of the intensity of that particular plane over the sum of the intensities of all the peaks within the 2θ range 20 to 80° [24]. The variation of the preferential orientation factor f(0 0 2) as a function of Zn doping level is presented in Fig. 2.

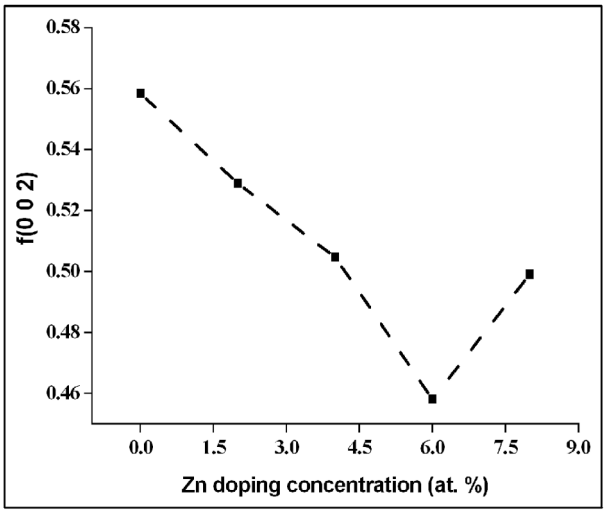

Fig. 2. Variation of the preferential orientation factor f(0 0 2) as a function of Zn doping level.

As can be seen from Fig. 2, f(0 0 2) decreases 6 at.% Zn doping concentration and then it increases with further Zn doping, suggesting a monotonic deterioration in the crystalline quality due to Zn doping. There are several possibilities, by which Zn^{2+} ions may be incorporated into the host CdS crystalline structure: Zn^{2+} ions may occupy interstitial positions in the CdS lattice, occupy empty locations of Cd^{2+} ions, or substitutionally replace Cd^{2+} ions. The low values of f(0 0 2) obtained for the films containing 6 at.% Zn doping might be due to the structural disorder introduced in the system due to the interstitially occupied Zn^{2+} ions. Above 6 at.% Zn doping concentration, Zn^{2+} ions enter the lattice both substitutionally and interstitially and, as a result, the f(0 0 2) value increases.

The lattice parameters, 'a' and 'c' are calculated using the formula of hexagonal system (equation 1):

$$\frac{1}{d^2} = \frac{4}{3}\frac{h^2 + hk + k^2}{a^2} + \frac{l^2}{c^2} \tag{1}$$

and the obtained values are presented in Table 1.

The small reduction of the lattice parameters of CdS:Zn films can be a consequence of the incorporation of Zn into the lattice. The ionic radii mismatch between Cd^{2+} and Zn^{2+} may be the cause for the reduction of lattice parameters of the doped films. This occurrence can happen when zinc ions enter substitutionally Cd sites. Similar results were obtained by Dzhafarov et al. [25] in CdS:In films deposited by spray pyrolysis technique. A shift of the (0 0 2) diffraction peak towards a high diffraction angle indicates the contraction in the CdS films with Zn doping.

The c/a ratio is found to be almost constant inferring that doping does not affect the fundamental structure of the undoped system, i.e. 'Zn' ion occupies the 'Cd' (metallic) site in the host lattice. The 'a' and 'c' values decrease with doping, keeping c/a constant. Fig. 3 shows the variation of a unit cell volume with Zn doping concentration.

As expected, the unit cell volume decreases with Zn doping due to the shift of (0 0 2) peak towards higher diffraction angle. This strongly supports for the successful replacement of Cd ions with smaller Zn ions.

The crystallite size (D) of Zn doped CdS films is calculated using the Scherrer formula [26]:

$$D = \frac{0.94\lambda}{\beta \cos\theta} \tag{2}$$

where λ is the wavelength of the X-ray used (1.5406 Å), β is the full width at half maximum of the strongest peak, and θ is the Bragg angle. Fig. 4 shows the variation of FWHM (β) and crystallite size (D) as a function of Zn doping concentration.

Table 1. 2θ, d-spacing values and structural parameters of undoped and Zn-doped CdS thin films.

Zn doping concentration (at.%)	2θ position for the (0 0 2) plane	Observed d-spacing (Å) for the (0 0 2) plane	Crystallite size, D (nm)	Lattice parameters* (Å)		c/a
				'a'	'c'	
0	26.497	3.3612	19.91	4.1166	6.722	1.6329
2	26.542	3.3555	20.93	4.1096	6.711	1.633
4	26.602	3.3481	17.49	4.1005	6.696	1.6329
6	26.610	3.3471	16.66	4.0883	6.694	1.6329
8	26.648	3.3428	16.33	4.0941	6.686	1.6331

*Standard values (JCPDS Card: 06-0314) a = 4.136 Å, c = 6.713 Å

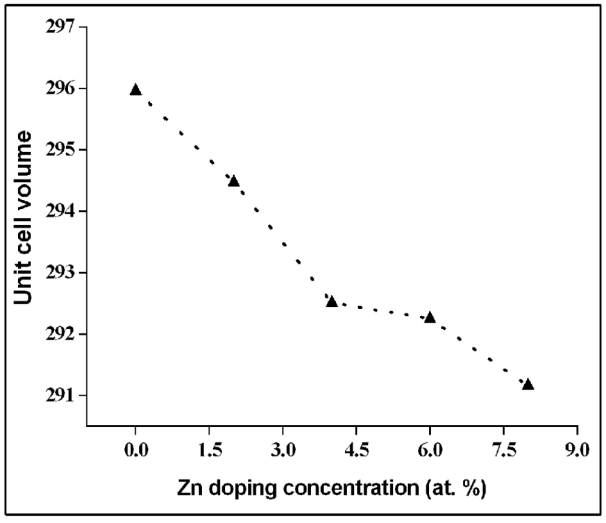

Fig. 3. Variation of a unit cell volume with Zn doping concentration.

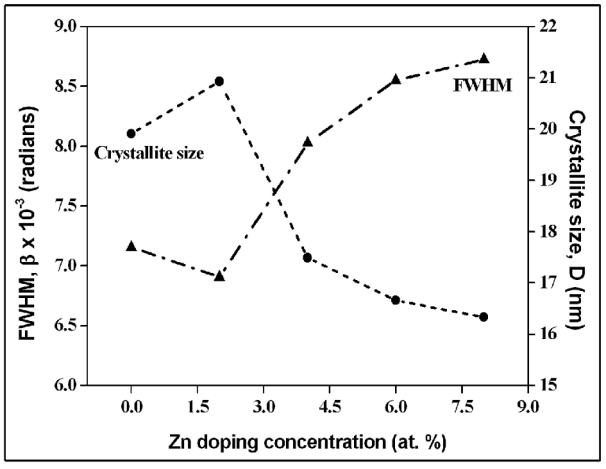

Fig. 4. Variation of FWHM (β) and crystallite size (D) as a function of Zn doping concentration.

It is observed that FWHM shows an increasing trend with Zn concentration whereas the crystallite size shows a decreasing trend, which is an expected result as the ionic radius of Zn is smaller (0.74 Å) than that of Cd (0.97 Å). The crystallite size declines gradually as the Zn doping level in the starting solution increases and attains a minimum value of 16.33 nm (Table 1). This decrease in crystallite size may be caused by the enhanced incorporation of Zn^{2+} ions into the Cd^{2+} sites. The minimum value of crystallite size obtained for the film coated with 8 at.% Zn doping confirms that there is an enhancement in Zn incorporation in the host lattice, which is well acknowledged from the elemental analysis (Section 3.3).

3.2. SEM analysis

The surface morphologies of undoped and Zn-doped CdS thin films are shown in Fig. 5.

Fig. 5a is the SEM image of undoped CdS thin film, which depicts the island growth on the film. Such island growth of undoped CdS film was reported by Chu et al. [27]. They attributed this growth to rapid nucleation and crystal growth of CdS due to a large number of free cadmium metal ions. The excess of Cd metal ions observed for the undoped CdS film (Table 2) strongly favors the island growth observed here. Fig. 5 (b – e) show the SEM images of the CdS thin films doped with 2, 4, 6 and 8 at.% Zn concentrations, respectively. With 2 at.% Zn doping, the surface is covered with nanosized grains scattered throughout the whole area (Fig. 5b). Traces of few fused nanosize grains can be found on the surface of the CdS film coated

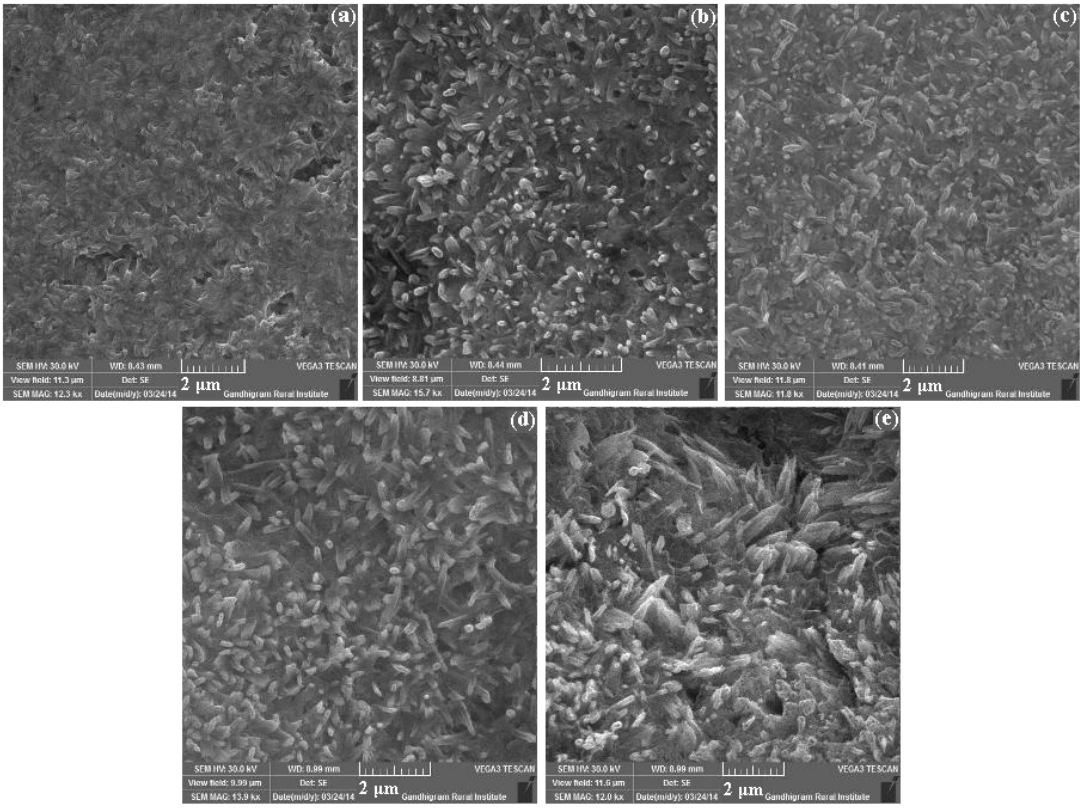

Fig. 5. SEM images of undoped and Zn-doped CdS thin films.

with 4 at.% Zn dopant (Fig. 5c). No fused grains are observed for the film coated with 6 at.% Zn dopant (Fig. 5d) and the surface appears to be homogeneous, uniform and compact. The film surface modifies to nanosized needle shaped grains for the film coated with 8 at.% Zn dopant, of which few grains are aligned perpendicular to the surface of the substrate (Fig. 5e). Thus, it can be concluded that as Zn doping increases, the film surface modifies from island growth formation to nanosized needle shaped grains.

Table 2. Elemental compositions of undoped and Zn-doped CdS thin films.

Zn doping concentration (at.%)	at.% Elements			
	Cd	S	Zn	Cl
0	47.20	46.54	–	6.26
2	47.98	44.39	2.65	4.98
4	48.59	43.14	3.41	4.86
6	48.79	42.67	3.96	4.58
8	48.88	41.38	4.73	5.01

3.3. Elemental analysis

The EDAX spectra of pure and Zn-doped CdS films are given in Fig. 6, which shows that pure CdS film contain the Cd and S elements whereas the doped films contain the Cd, S and Zn elements as it has been expected.

The other elements (Ca, Na, Si and Cl) that are not expected to be in the deposited films may stem from the glass substrates [28]. The quantitative results presented in Table 2 show that for pure CdS (0 at.% Zn) film, S/(Cd+Zn) atomic ratio is ∼1 confirming the perfect stoichiometric nature of this film.

When Zn doping concentration increases, the stoichiometric nature detoriates as (Cd + Zn) composition increases and S value decreases. Thus, it

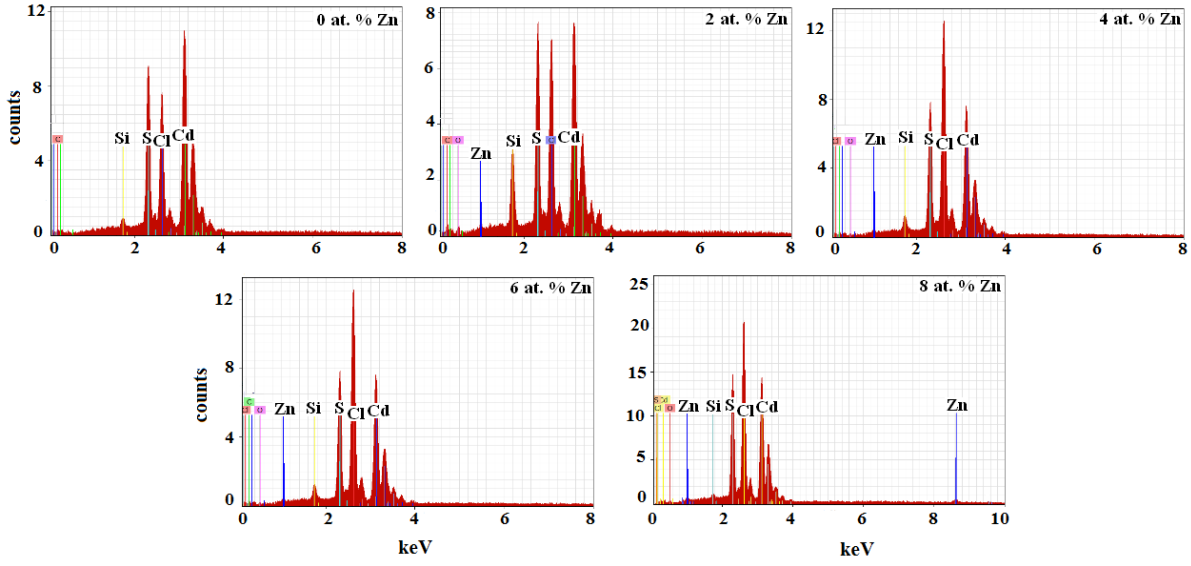

Fig. 6. EDAX spectra of undoped and Zn-doped CdS thin films.

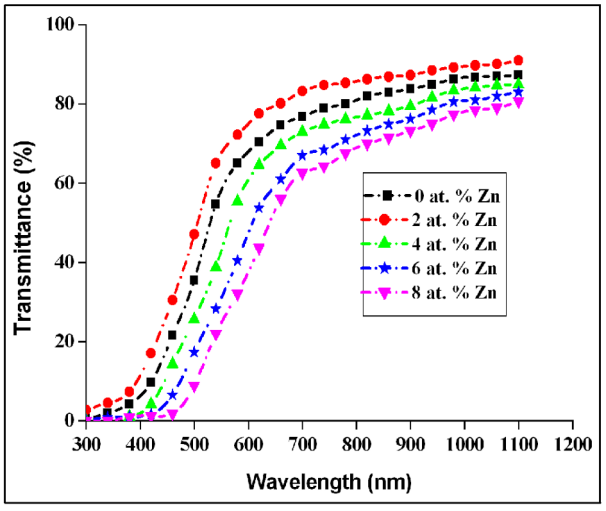

Fig. 7. Transmittance spectra of undoped and Zn-doped CdS thin films.

is evident that the number of sulfur vacancies increases as Zn doping concentration increases and this might be the reason for the decreased sheet resistance values obtained for the doped films as it is shown in Section 3.5.

3.4. Optical studies

Transmission spectra of pure and Zn doped CdS films are shown in Fig. 7.

All the films show very high transmittance in the visible and near-IR regions and the film coated with 2 at.% Zn concentration shows a transmittance nearly equal to 85 % at 600 nm. The high transmittance of the films is an indication for their improved crystalline nature and high degree of stoichiometry. A blue shift in the absorption edge is observed for the film coated with 2 at.% Zn doping concentration and a red shift is observed for the films coated with higher Zn doping concentration. Optical band gap E_g of the films can be estimated from the Tauc plot [29]:

$$(\alpha h\gamma) = A\,(h\gamma - E_g)^n \qquad (3)$$

where E_g is the band gap corresponding to a particular transition occurring in the film, A is the band edge constant, γ is the transition frequency, and the exponent n characterizes the nature of band transition. For crystalline semiconductors, n can take the values $\frac{1}{2}$, $\frac{3}{2}$, 2 or 3 when the transitions are direct allowed, direct forbidden, indirect allowed and indirect forbidden, respectively. The band gap E_g can be obtained from the extrapolation of the straight line portion of the $(\alpha h\gamma)^{\frac{1}{n}}$ vs. $h\gamma$ plot (Fig. 8) to $h\gamma = 0$.

The estimated band gap values are presented in Table 3. The band gap value of undoped CdS film

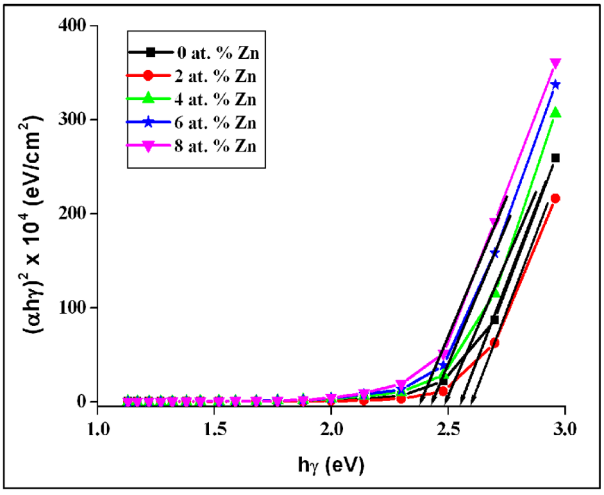

Fig. 8. Plots of $(\alpha h\gamma)^{\frac{1}{2}}$ vs. $h\gamma$ for the CdS films.

was found to be equal to 2.42 eV. This value exactly matches with the value obtained by Shah et al. [30]. It is also observed that the band gap initially decreases with Zn doping concentration up to 2 at.% and then starts to increase with higher Zn doping concentration. The enhancement in band gap of CdS thin films with Zn doping concentration greater than 2 at.%, in which the crystallite size decreases (Table 1), can be related to quantum confinement effect [31].

In doped semiconductors, there is a possibility of widening of optical band gap due to Burstein-Moss (BM) effect [32], which takes place as a result of an increase in their carrier concentration. This is well supported by the low sheet resistance values obtained for the films coated with Zn doping concentration greater than 2 at.% (Table 3) as R_{sh} is inversely proportional to the carrier concentration. The increase in carrier concentration indicates that most of the Zn^{2+} substitutes uniformly for Cd^{2+} in the host lattice. The decreased band gap value obtained for the CdS film coated with 2 at.% Zn dopant may be due to the Zn defect states originated within the forbidden gap, which may lead to absorption of incident photons and a substitutional dissolution, which yield an improvement in the crystalline quality of this film [33]. This is well supported by the large value of crystallite size obtained for this film (Table 1). The wide band gap and high optical transparency in the visible range observed for the doped films make them possible window layers in solar cells.

3.5. Electrical studies

The variation in electrical sheet resistance (R_{sh}) of the CdS:Zn films as a function of Zn doping level in the starting solution is shown in Fig. 9 and the corresponding resistivity (ρ) values are presented in Table 3.

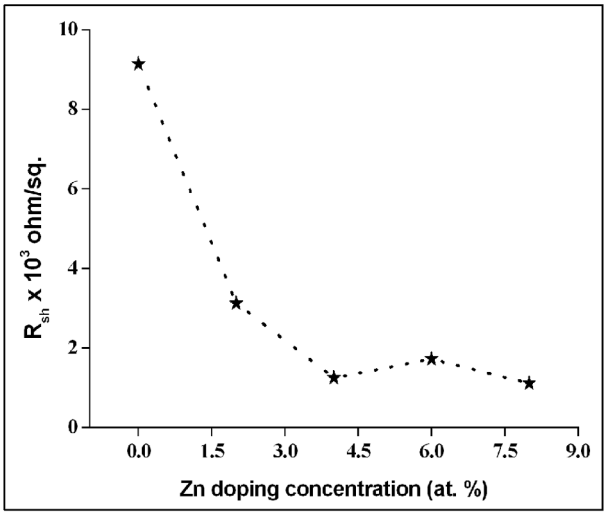

Fig. 9. Variation in electrical sheet resistance (R_{sh}) of the CdS:Zn films as a function of Zn doping level.

The R_{sh} decreases slowly as the doping level increases, attaining a minimum value ($1.113 \times 10^3 \Omega$/sq) for the film coated with 8 at.% Zn dopant. The undoped film has a resistivity of 5.01×10^{-3} Ω·cm and it reduces to a minimum of 0.574×10^{-3} Ω·cm for 8 at.% Zn doped film. The obtained value of resistivity for undoped CdS exactly matches with the value presented by Khallaf et al. [8] for gallium doped CdS thin films grown by chemical bath deposition. Generally, the resistivity of Zn-doped CdS films depends on the following factors: (i) interstitial incorporation of Zn, (ii) presence of sulfur vacancies and (iii) substitutional incorporation of Zn^{2+} ions in the Cd sites. The decrease in resistivity values of CdS films with Zn-doping might be due to the increased carrier concentration obtained for these films. This

Table 3. Optical and electrical parameters of undoped and Zn-doped CdS thin films.

Zn doping concentration (at.%)	T %	Optical band gap energy, E_g (eV)	Sheet resistance, $R_{sh} \times 10^3$ Ω/sq	Resistivity, $\rho \times 10^{-3}$ Ω·cm
0	87.28	2.42	9.143	5.01
2	90.98	2.38	3.124	1.759
4	84.98	2.49	1.252	0.7568
6	83.02	2.56	1.724	1.1206
8	80.67	2.6	1.113	0.574

is strongly supported by the decreased d-values observed for the film with Zn doping (Table 1). Sulfur vacancies also play a role in the resistivity of the CdS films. Elemental analysis (Section 3.3) shows that as the Zn doping concentration increases, sulfur content in the films decreases. The increased sulfur vacancies cause an increase in the carrier concentration of the films, hence, the sheet resistance is decreased. Thus, it can be concluded that sulfur vacancies and substitutional incorporation of Zn^{2+} ions in the Cd sites enhances the electrical conductivity of CdS:Zn films.

4. Conclusions

Good crystalline quality CdS:Zn thin films were deposited by spray pyrolysis technique using a perfume atomizer with different doping levels (0, 2, 4, 6 and 8 at.%) of Zn. The physical properties of the films were analyzed to understand the influence of Zn doping level. From the XRD studies, it was confirmed that the obtained CdS:Zn films had a hexagonal phase with (0 0 2) preferential orientation. The crystallite size of CdS films was found to decrease from 20.93 nm to 16.33 nm with the increase in Zn doping level. The optical studies revealed that all the films showed good transmittance of about 80 %. The surface modification from island growth to uniformly distributed nano sized grains observed in the SEM images clearly suggested that the amount of Zn doping had an important influence on the surface morphology of the CdS films. Resistivity value decreased as Zn doping concentration increased and a minimum resistivity of 0.574×10^{-3} Ω·cm was observed for the film coated with 8 at.% Zn dopant. Thus, the film coated with 8 at.% Zn dopant had better structural, morphological and electrical properties. High optical transmittance, large band gap in the visible range and low resistivity values obtained for CdS:Zn thin films make them a promising candidate for optoelectronic devices as well as the window/buffer layer materials in heterojunction photovoltaic cells.

Acknowledgements

The authors are grateful to the Secretary and Correspondent, AVVM Sri Pushpam College (Autonomous), Poondi, for his excellent encouragement and support to carry out this work.

References

[1] KAR S., CHAUDHURI S., *Synth. React. Inorg. M.*, 36 (2006), 289.
[2] AFIFY H.H., BATTISHA I.K., *J. Mater. Sci.-Mater. El.*, 11 (2000), 373.
[3] UDA H., SONOMURA H., IKEGAMI S., *Meas. Sci. Technol.*, 8 (1997), 86.
[4] LIU Y.K., ZAPIEN J.A., GENG C.Y., SHAN Y.Y., LEE C.S., LIFSHITZ Y., LEE S.T., *Appl. Phys. Lett.*, 85 (2004), 3241.
[5] DUAN X., HUANG F.Y., AGARWAL R., LIEBER C.M., *Nature*, 421 (2003), 241.
[6] ACOSTA D., MAGANA C., MARTINEZ A., MALDONADO A., *Sol. Energ. Mat. Sol. C.*, 82 (2004), 11.
[7] PATIL B., NAIK D., SHRIVASTAVE V., *Chalcogenide Lett.*, 8 (2011), 117.
[8] KHALLAF H., CHAI G., LUPAN O., CHOW L., PARK S., SCHULTE A., *Appl. Surf. Sci.*, 255 (2009), 4129.
[9] LEE J., YI J., YANG K., PARK J., OH R., *Thin Solid Films*, 431 (2003), 344.
[10] BACAKSIZ E., TOMAKIN M., ALTULBAS M., PARLAK M., COLAGOKLU T., *J. Phys.-Condens. Mat.*, 403 (2008), 3740.
[11] CHANDRAMOHAN S., STRACHE T., SARANGI S., SATHYAMOORTHY R., SOM T., *Mater. Sci. Eng. B-Adv.*, 171 (2010), 16.

[12] SATHYAMOORTHY R., SUDHAGAR P., BALERNA A., BALASUBRAMANIAN C., BELLUCCI S., POPOV A.I., ASHOKAN K., *J. Alloy. Compnd.*, 493 (2010), 240.
[13] SAHAY P.P., NATH R.K., TEWARI S., *Cryst. Res. Technol.*, 42 (2007), 275.
[14] ASHOUR A., *Turk. J. Phys.*, 17 (2003), 551.
[15] TOMITA Y., KAWAI T., HATANAKA Y., *Jpn. J. Appl. Phys.*, 33 (1994), 3383.
[16] ULLRICH B., SAKI H., SEGAWA Y., *Thin Solid Films*, 385 (2001), 220.
[17] BOIERIU P., SPORKEN R., XIN Y., BROWNING N., SIVANANTHAN S., *J. Electron. Mater.*, 29 (2000), 718.
[18] PRADHAN B., SHARMA A.K., RAY A.K., *J. Cryst. Growth*, 304 (2007), 388.
[19] ILIEVA M., DIMOVA-MALINOVSKA D., RANGUELOV B., MARKOV I., *J. Phys. Condens. Mater.*, 11 (1999), 10025.
[20] ATAY F., BILGIN V., AKYUZ I., KOSE S., *Mater. Sci. Semicond. Process.*, 6 (2003), 197.
[21] ANBARASI M., NAGARETHINAM V.S., BALU A.R., *Int. J. Chem. Phys. Sci.*, 3 (2014), 1.
[22] SIVARAMAN T., NAGARETHINAM V.S., BALU A.R., *J. Mater. Sci. Res.*, 2 (2014), 6.
[23] WILSON K.C., MANIKANDAN E., BASHEE AHAMED M., MWAKIKUNGA B.W., *J. Alloy. Compd.*, 585 (2014), 555.
[24] BALU A.R., NAGARETHINAM V.S., SUGANYA M., ARUNKUMAR N., SELVAN G., *J. Electr. Dev.*, 12 (2012), 739.
[25] DZHAFAROV T.D., ONGUL F., AYDIN YUKSEL S., *Vacuum*, 84 (2010), 310.
[26] NARASIMMAN V., NAGARETHINAM V.S., BALU A.R., SUGANYA M., ANBARASI M., USHARANI K., *Int. J. Appl. Res. Eng. Sci.*, 1 (2014), 7.
[27] CHU J., JIN Z., CAI S., YANG J., HONG Z., *Thin Solid Films*, 520 (2012), 1826.
[28] USHARANI K., BALU A.R., SHANMUGAVEL G., SUGANYA M., NAGARETHINAM V.S., *Int. J. Sci. Res. Rev.*, 2 (2013), 53.
[29] RAJASHREE C., BALU A.R., NAGARETHINAM V.S., *Int. J. ChemTech Res.*, 6 (2014), 347.
[30] SHAH N.A., SAGAR R.R., MAHMOOD W., SYED W.A.A., *J. Alloy. Compd.*, 512 (2012), 185.
[31] WANG Y.G., LAU S.P., LEE H.W., LU S.F., TAY S.K., ZANG X.Z., HING H.H., *J. Appl. Phys.*, 94 (2003), 354.
[32] VINODKUMAR R., LETHY K.J., ARUNKUMAR P.R., RENJU KRISHNAN R., VENUGOPALAN PILLAI N., MAHADEVAN PILLAI V.P., PHILIP R., *Mater. Chem. Phys.*, 121 (2010), 406.
[33] KOSE S., ATAY F., BILGIN V., AKYUZ I., KETENCI E., *Appl. Surf. Sci.*, 256 (2010), 4299.

Received 2014-06-28
Accepted 2014-08-31